

Multilayered optical data storage using a spatial soliton

Masaki Hisaka^{a)} and Kosuke Yoshida

Department of Electronics and Lightwave Sciences, Osaka Electro-Communication University, Neyagawa, Osaka 572-8530, Japan

(Received 14 October 2008; accepted 26 November 2008; published online 16 December 2008)

Multilayered optical data storage using a spatial soliton, which has the potential to increase the number of recording layers, is proposed and experimentally investigated. A Ti:sapphire pulsed laser focusing near the surface of a Ce-doped $\text{Sr}_{0.75}\text{Ba}_{0.25}\text{Nb}_2\text{O}_6$ crystal generated a second-harmonic (SH) beam associated with the self-focusing fundamental laser and induced SH collision responses to the counterpropagating laser pulses. Using threshold controls, single-bit data were recorded with a domain-reversal technique at the collision point, and its data were read out through a quasi-phase-matched SH generation process enhanced at the reversed domains. Multilayered recording and selective data rerecording were also demonstrated. © 2008 American Institute of Physics. [DOI: 10.1063/1.3050454]

Multilayered optical data storage¹⁻³ is interesting for developing high-density optical data storage systems. Such systems record data in three dimensions using a highly focused laser beam spot and can achieve data storage densities higher than a single layer system. However, the main difficulties are spherical aberration and short working distance of the focusing lens when the laser beam is focused at deep areas. This restricts the number of recording layers because it is difficult to record bit data at deep layers. To address these difficulties, we propose a multilayered optical data storage using a spatial soliton that will greatly increase the number of recording layers.

Figure 1 shows the principle of multilayered optical data storage using a spatial soliton. This system focuses laser beams near the surface of the nonlinear recording media to produce an optical spatial soliton propagating in the depth direction (z -direction) to avoid the main difficulties associated with multilayered optical data storage systems. The spatial soliton enables high-density optical recording deep into recording media because the beam width remains constant at all z positions. Data recording is accomplished by the collision effects of counterpropagating (CP) laser pulses. Physical or chemical change in the media is induced by nonlinear optical interactions at the pulse collision point. The lateral and axial bit sizes are determined by the spatial soliton beam width and the laser pulse width, respectively. Multilayered recording is performed by changing collision points in three dimensions. If the formation condition of the spatial soliton is not affected by optical losses such as photoabsorption and light scattering, we can achieve multilayered optical data storage with theoretically no limit to the media thickness and number of recording layers because the spatial soliton can propagate infinitely.

Such optical data recording is realized by three elemental technologies: (i) formation of an optical spatial soliton in the recording media, (ii) nonlinear optical collision response of CP laser pulses, and (iii) physical or chemical change in the media at the collision point. To investigate these technologies, we selected a strontium barium niobate (SBN) crystal as a storage medium. The crystal, with excellent pho-

torefractivity and relaxor ferroelectricity,⁴ has been used in studying holographic recording,^{5,6} optical spatial solitons,⁷ domain reversal,^{3,5,6,8-12} second-harmonic generation (SHG),⁸⁻¹² and CP response.¹²⁻¹⁴ In the present study, a cerium-doped SBN:75 (Ce:SBN:75) crystal was used for its effective photoabsorption. It has a Curie temperature (T_C) of ~ 56 °C and coercive electric field (E_C) of ~ 0.7 kV/mm.

A Ti:sapphire ultrashort pulsed laser (CDP Systems Corp., Tissa-20), with a pulse width, central wavelength, average optical power, and repetition rate of 55 fs, 800 nm, 240 mW, and 80 MHz, respectively, was divided into two beams to irradiate a Ce:SBN:75 crystal having dimensions of $3 \times 4 \times 5$ mm³ from both sides (Fig. 2). The CP lasers were individually focused near the crystal surface with a numerical aperture of 0.08. The laser path lengths were adjusted to meet the CP pulses in the crystal. The polarization of the laser beam and c -axis of the crystal coincided with the x -axis, where x , y , and z axes are defined in Fig. 2. A Peltier element (PE) controls the crystal temperature T , and an external electric dc field E is applied parallel to the polar c -axis. The collision point of the CP pulses along the z - and x -directions was controlled by optical delay in one optical path and by scanning the crystal, respectively. The beams

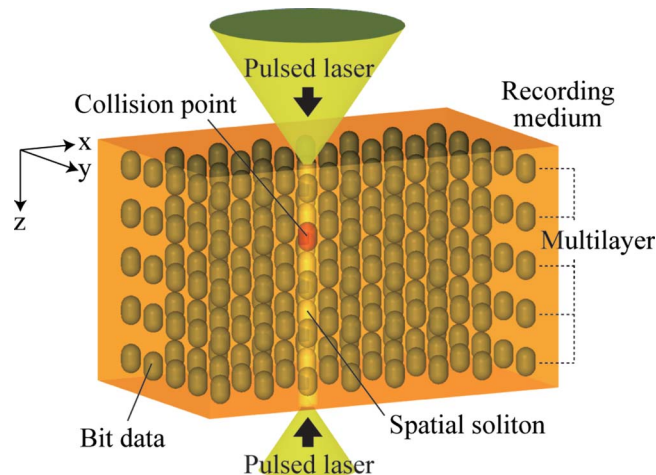


FIG. 1. (Color online) Multilayered optical data storage using a spatial soliton.

^{a)}Electronic mail: hisaka@isc.osakac.ac.jp.

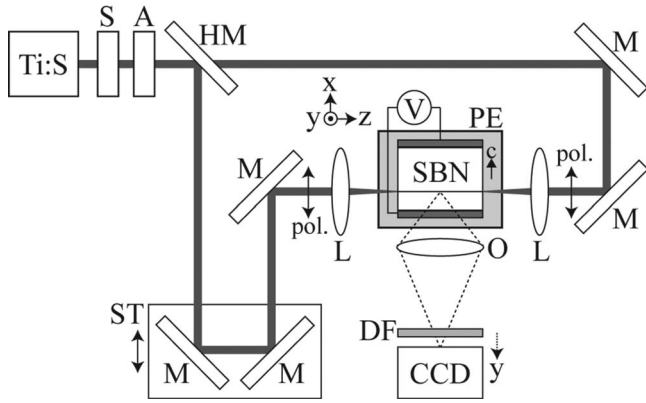


FIG. 2. Experimental setup: Ti:S, Ti:sapphire laser; SBN, SBN crystal; CCD, charge-coupled device camera; PE, Peltier element; DF, dichroic filter; ST, stage; S, shutter; A, aperture; HM, half-mirror; M, mirror; O, objective; L, lens. The CCD camera captured the beam images from the *y*-direction normal to the crystal *c*-axis.

propagating within the crystal were observed through a dichroic filter (DF) using a charge-coupled device (CCD) camera situated along the *y*-direction, perpendicular to the crystal *c*-axis.

First, the formation of the optical spatial soliton was investigated. High intensity Ti:sapphire laser pulses produced the fundamental beam (FB) and its SH beam (SHB) within the crystal. The SHB is formed by the SH radiation emitted in a plane perpendicular to the crystal *c*-axis. We observed only the SHB to examine the nonlinear optical effects at the collision point. Figure 3(a) shows the SHB image when the fundamental pulsed laser was irradiated from the left side at $T=25\text{ }^\circ\text{C}$ and $E=0.0\text{ kV/mm}$. The full widths at half maximum (FWHMs) of the transverse beam profile (*x*-direction) are $8.4\text{ }\mu\text{m}$ at $z=z_1$ and $7.1\text{ }\mu\text{m}$ at $z=z_2$ [Fig. 3(b)]. The beam width of the SHB remains almost constant at a distance of $400\text{ }\mu\text{m}$ ($=z_2-z_1$), which is associated with the self-focusing process for the FB.¹¹ We verified in a previous experiment that the SHB width was almost constant over about 1 mm distance. The shorter distance observed in this experiment is due to optical loss by scattering and photoabsorption of the FB and SHB.

Using the SHB, we investigated the optical collision responses of the CP pulses. When the pulsed laser was irradiated from both sides, a stable CP self-trapped beam was ob-

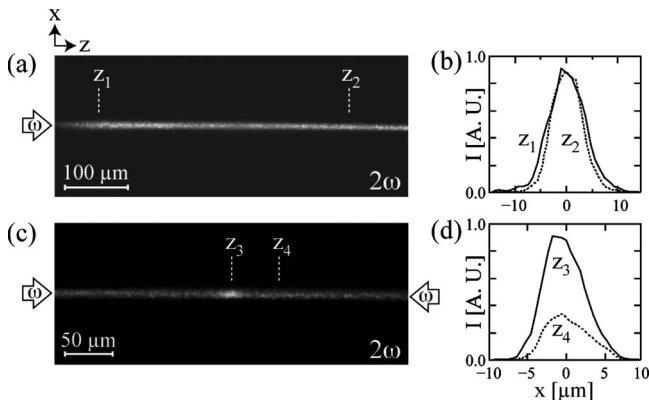


FIG. 3. SHB and collision of CP laser pulses. (a) SH beam associated with the self-focusing FB. (b) Lateral beam profiles of SHB at $z=z_1$ and $z=z_2$ in (a). (c) SH collision response. (d) Lateral beam profiles of collision point at $z=z_3$ and noncollision point $z=z_4$ in (c).

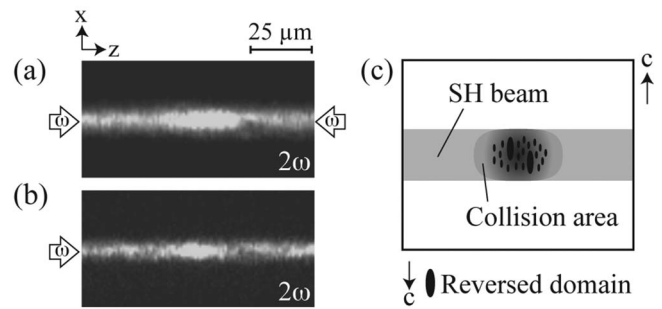


FIG. 4. Bit data recording and its reading. (a) Recording process of bit data at the collision point of CP laser pulses. (b) Readout of the recorded data by SHG enhancement. (c) A schematic of reversed domains recorded in the collision area.

served in the SBN crystal even though instable CP spatial solitons in bulk media were reported in earlier works.^{13,14}

Figure 3(c) shows the CP beam and SH collision responses of the CP pulses. The SH intensity is enhanced at the collision point ($z=z_3$). The position of $z=z_4$ corresponds to the noncollision point, which is located $50\text{ }\mu\text{m}$ from $z=z_3$. Figure 3(d) shows the transverse beam profile at $z=z_3$ and $z=z_4$. The FWHMs of the SHB width and SH intensity are $6.3\text{ }\mu\text{m}$ and 0.34 at $z=z_3$, and $6.5\text{ }\mu\text{m}$ and 0.91 at $z=z_4$, respectively. The beam widths at $z=z_3$ are 0.97 times smaller, and the intensities are 2.7 ($=0.91/0.34$) times larger than those at $z=z_4$. The optical response at the collision point of the SHB exhibited nonlinear behavior in the SH intensity.

To record bit data at the collision point, we attempted to reverse the small domains (size, $1\text{--}8\text{ }\mu\text{m}$), which are known to build a random ferroelectric domain structure, at the collision point by threshold control of T and E . Initially, the SBN crystal is electrically poled at $T=50\text{ }^\circ\text{C}$ and $E=+0.7\text{ kV/mm}$ for $\Delta t=30\text{ s}$. Then, it is cooled to $T=25\text{ }^\circ\text{C}$. To reverse the crystal domains at the collision position, a negative field E of -0.2 kV/mm was applied for $\Delta t=0.5\text{ s}$. Figure 4(a) shows a SH intensity image during the depoling process. The axial beam profile of the SH beam at the collision point is $29.7\text{ }\mu\text{m}$ in the FWHM. Next, the locally disordered domains were inspected by laser pulse irradiation from the left side of the crystal at $E=0.0\text{ kV/mm}$. Figure 4(b) shows a SH intensity image, in which SH enhancement is observed at the collision point. The enhancement process is explained by the quasi-phase-matching, which is provided where the domain structure relaxed to a randomized state due to local heating.^{8,10,11} The axial beam profile corresponding to the collision position is $19.3\text{ }\mu\text{m}$ FWHM and is reduced by a factor of 0.65 . This reduced intensity profile indicates that the reversed small domains are effectively absorbed by cerium atoms doped in the SBN crystal, resulting in a local increase in the crystal temperature. The small domains were reversed at the local area where $E>E_c$. Figure 4(c) shows a schematic of reversed domains formed within a collision area. Single-bit data are recorded as an aggregate of the reversed small domains.

With this domain-reversal technique, multilayered recording was realized by changing the collision point along the *x*- and *z*-directions. First, we investigated lateral recording at $z=z_5$. To reverse the aggregate of small domains at three different *x* positions with the bit interval of $300\text{ }\mu\text{m}$,

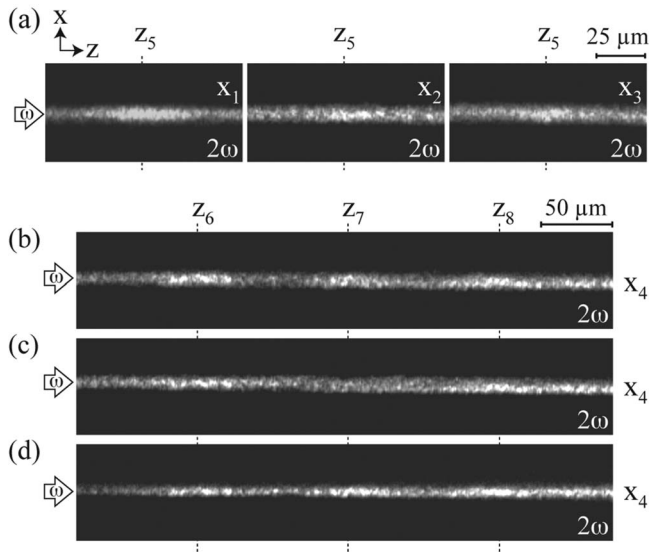


FIG. 5. Multilayered optical data storage and selective data rerecordability. (a) Lateral data recording at the different positions of $x=x_1$, x_2 , and x_3 . (b) Axial data recording at the different positions of $z=z_6$, z_7 , and z_8 . (c) Selective bit data erasing at $(x, z)=(x_4, z_7)$. (d) Rerecording bit data at the erased position of $(x, z)=(x_4, z_7)$.

the negative field $E=-0.2$ kV/mm was successively applied for $\Delta t=0.5$ s when the collision point is located at each position. Then each data were read out by irradiating the fundamental pulsed laser from the left side of the crystal. Figure 5(a) shows readout images recorded at $x=x_1$, x_2 , and x_3 , where the SH intensities are enhanced. We also investigated axial recording at $x=x_4$. With similar E and Δt , the local domain reversals were successively performed at $z=z_6$, z_7 , and z_8 with the distance of $100 \mu\text{m}$ between neighboring layers. When the pulsed laser was irradiated from the left side of the crystal, the SH intensities were simultaneously enhanced at each position [Fig. 5(b)]. However, the signal to noise ratio (SNR) decreased, which suggests that a small amount of reversed domain was also generated at the non-collision area, and the cross-talk reduced the SNR in multilayered recording.

Then, to investigate selective data erasing, a positive field E of $+0.2$ kV/mm was applied for $\Delta t=0.1$ s when the collision point was at $(x, z)=(x_4, z_7)$. Figure 5(c) shows that the SH intensity at $z=z_7$ decreased slightly when the crystal was irradiated from the left side at $E=0.0$ kV/mm. The positive external electric field reduced the number of reversed domains. When an appropriate threshold is set between the recording bit and erased bit signals, the bit data at

$z=z_7$ can be regarded as erased data. Further, to investigate rerecordability of the system, we tried to rerecord bit data at the erased position of $z=z_7$. A field of $E=-0.2$ kV/mm was applied for $\Delta t=0.5$ s when the collision point was at $z=z_7$. The SH intensity is enhanced again at $z=z_7$ where the reversed crystal domains are reproduced [Fig. 5(d)]. This technique can provide rerecordable multilayered optical data storage.

We have proposed multilayered optical storage using a spatial soliton and demonstrated basic experiments of multilayered bit recording, reading, erasing, and rerecording. These effects are operative at the collision point of CP laser pulses using domain reversal in a Ce-doped SBN:75 crystal. The experimental results can lead to important techniques of axial local photon control of high spatial resolution deep inside materials. However, many issues remain to be addressed in this optical data storage system. In the future, we should investigate (1) bit size reduction, (2) decrease in bit and layer intervals, (3) a shorter recording process, (4) organic materials as recording media, (5) SHG reduction in the noncollision areas, (6) increase in number of recording layers, (7) SNR enhancement, and (8) coaxial bit data and lateral parallel data reading. Further, the physical mechanism of SH optical responses of CP laser pulses and the interaction between the response and media should be investigated in detail.

¹D. A. Parthenopoulos and P. M. Rentzepis, *Science* **245**, 843 (1989).

²J. H. Strickler and W. W. Webb, *Opt. Lett.* **16**, 1780 (1991).

³M. Hisaka, H. Ishitobi, and S. Kawata, *J. Opt. Soc. Am. B* **17**, 422 (2000).

⁴A. S. Bhalla, R. Guo, L. E. Cross, G. Burns, F. H. Dacol, and R. R. Neurgaonkar, *J. Appl. Phys.* **71**, 5591 (1992).

⁵F. Micheron and G. Bismuth, *Appl. Phys. Lett.* **23**, 71 (1973).

⁶A. S. Kewitsch, M. Segev, A. Yariv, G. J. Salamo, T. W. Towe, E. J. Sharp, and R. R. Neurgaonkar, *Phys. Rev. Lett.* **73**, 1174 (1994).

⁷G. Duree, M. Morin, G. Salamo, M. Segev, B. Crosignani, P. D. Porto, E. Sharp, and A. Yariv, *Phys. Rev. Lett.* **74**, 1978 (1995).

⁸M. Horowitz, A. Bekker, and B. Fischer, *Appl. Phys. Lett.* **62**, 2619 (1993).

⁹A. S. Kewitsch, T. W. Towe, G. J. Salamo, A. Yariv, M. Zhang, M. Segev, E. J. Sharp, and R. R. Neurgaonkar, *Appl. Phys. Lett.* **66**, 1865 (1995).

¹⁰A. R. Tunyagi, M. Ulex, and K. Betzler, *Phys. Rev. Lett.* **90**, 243901 (2003).

¹¹R. Fischer, S. M. Saitiel, D. N. Neshev, W. Krolikowski, and Y. S. Kivshar, *Appl. Phys. Lett.* **89**, 191105 (2006).

¹²R. Fischer, D. N. Neshev, S. M. Saitiel, A. A. Sukhorukov, W. Krolikowski, and Y. S. Kivshar, *Appl. Phys. Lett.* **91**, 031104 (2007).

¹³M. Petrovic, D. Jovic, M. Belic, J. Schröder, Ph. Jander, and C. Denz, *Phys. Rev. Lett.* **95**, 053901 (2005).

¹⁴P. Jander, J. Schröder, C. Denz, M. Petrovic, and M. R. Belic, *Opt. Lett.* **30**, 750 (2005).